Lattice Gas Models : Flow, Porous Media, and Bubbles.

Peter Stuart

July 10, 2002

Abstract

The validity of Lattice Gas Models is assessed using some simple experiments. Flow through a channel and flow past a barrier at different Reynolds number are simulated. Flow through porous media is investigated and the critical exponent μ defined by the dependence of the current density J on porosity ϕ was found using finite scaling to be 1.288 ± 0.084. The Lattice Gas is used to construct a bubble which is shown to obey Laplace's Law and deform in fluid flow.

Acknowledgments

I would sincerely like to thank my project supervisor Stefan Hutzler for his help and guidance during this project. I would also like to thank all my fellow undergraduates who gave me much support and advice over the last couple of very difficult months.

Contents

1 Introduction

Fluid dynamics, the study of moving fluids is very important as fluids are everywhere in the everyday world. Fluids include liquids and gases, air and water are common examples. The applications of fluid dynamics are far reaching from the study of air resistance or drag on a sports car to the flow of blood through the body. This project uses Lattice Gas Cellular Automata (Lattice Gas Models) as means of performing fluid dynamics calculations computationally.

1.1 Lattice Gas Models

The flow of fluids are traditionally described by the Navier-Stokes Equation (1). This is an example of a nonlinear partial differential equation, which are difficult to solve typically requiring sophisticated numerical methods. Lattice gas models came into being out of a desire to simulate fluid flow without having to tackle the Navier-Stokes Equation [1].

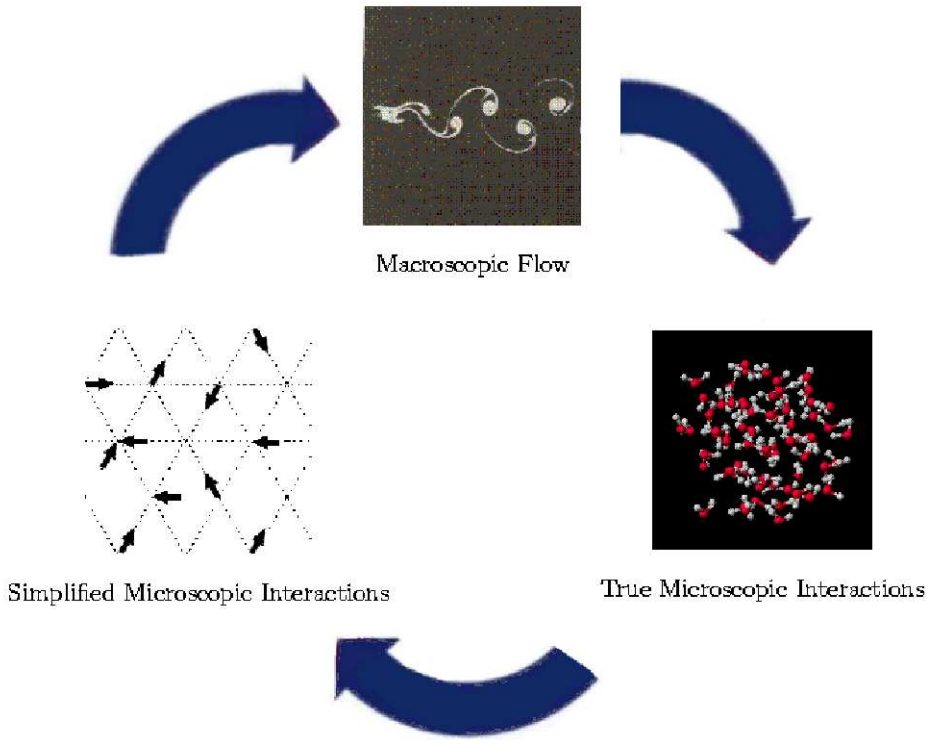

Figure 1: The principle behind Lattice Gas Models.

The principle behind lattice gas models is that if the essential features of real fluid are maintained at a microscopic scale then the correct physical behavior will

be reproduced at a macroscopic level [2]. This means that the complex interactions of the particles that make up a fluid can be vastly simplified and still produce the correct results (Figure 1). Considering the Navier-Stokes Equation (1) at a microscopic level suggests two basic ingredients for such a model

- Local conservation of particles at each time step.
- Local conservation of momentum at each time step.

Lattice Gas models are a form of cellular automata (CA). Basically a CA is a regular arrangement of cells each containing a finite number of states. All cells are updated simultaneously using a set of predetermined rules which depend on the local neighborhood of cells only. The classic example of a CA is the Game of Life introduced by Conway in the early 1970's[3]. In Lattice Gas Cellular Automata

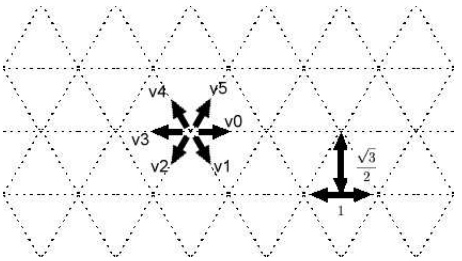

Figure 2: The triangular lattice and velocity vectors of the FHP model.

(LGCA) the positions of particles are restricted to sites on a lattice, and velocities are limited to a small number of velocity vectors. The primary LGCA which will be considered are the FHP model and its variants. The FHP model is characterized as follows [3]

- A triangular lattice of nodes which are each linked to six nearest-neighbors.
- A cell is associated with each link at every node (6 cells per node).
- Cells can be occupied by at most one particle (one boolean value).
- All particles have the same mass (set to 1 for simplicity).
- The evolution with time proceeds according to a set of predetermined rules which obey conservation of particles and conservation of momentum at each step.
- The update rules (collisions) are strictly local, only particles of a single node are involved.

Some variations of this model also contain a rest particle (eg. FHP-III) in which case there are seven cells associated with each node. The first lattice gas was the HPP model proposed by Hardy, de Pazzis and Pomeau in 1973. This model consisted of a square lattice and four primitive velocity vectors, however this model does not have sufficient symmetry to reproduce the Navier-Stokes equation in the macroscopic limit. The FHP model, proposed by Frisch, Hasslacher and Pomeau in 1986 with its greater (hexagonal) symmetry was the first to yield the Navier-Stokes equation in the macroscopic limit. The update process for this model consists of:

1. **Free motion between collisions** : The particles move in the direction of their velocity to a neighboring node, Figure 3 (a) → 3 (b).
2. **Collisions** : The velocities o each node are changed according to the predetermined collision rules, Figure 3 (b) → Figure 3 (c).

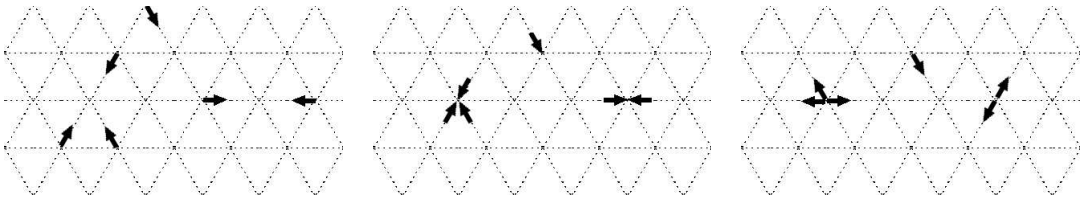

(a) Initial (b) Translate (c) Collision

Figure 3: Update process of the FHP Lattice Gas.

It is possible to predetermine the collision rules as there is a finite number of combinations of velocities that can occur at a node and hence a finite number of collision types which can occur. Only a few collisions give a non-trivial result (i.e. a collision in which the directions of motion have changed). This is computationally advantageous as the collision rules are worked out once, stored in computer memory, and accessed each time the lattice is updated. There is some flexibility in the choice of rules but they must reflect the local conservation of momentum and particle number at each time step expressed by the Navier-Stokes Equation (1). The detailed nature of the microscopic interactions does not affect the form of the equations but only the values of the coefficients (such as the viscosity) appearing in them [2].

1.2 Computational Implementation

As stated previously the FHP cellular automata consists of a triangular lattice. Each lattice node or site having either six or seven cells associated with it depending

on whether or not the model possesses a rest particle. Assuming we have a rest particle, seven boolean values are needed to describe the state of any lattice site at a particular time. In order to achieve efficient memory usage we use the first seven bits (labeled 0-6) of a variable which is of integer data-type [1]. The eighth bit (bit 7) is used to represent a (fixed) barrier site.

Cell		6	5	4	3	2	1	0
	rest	barrier	v_5	v_4	v_3	v_2	v_1	v_0
	■	●	↗	↖	←	↙	↘	→
Bit	7	6	5	4	3	2	1	0

Table 1: Storing information about a lattice site

The size of the integer data-type is four bytes so in principle one integer could be used to describe four lattice sites. This approach has not been taken to simplify programming, rather one integer describes one lattice site, hence an array of 1000 integers stores information about 1000 lattice sites. The spare bytes are not without use and are put to work in Section 4 when describing moving barrier sites. Consider a lattice site which contains velocities v_0, v_2, and v_4

Cell		6	5	4	3	2	1	0
	barrier	rest	v_5	v_4	v_3	v_2	v_1	v_0
				↖		↙		→
Boolean	0	0	0	1	0	1	0	1

Table 2: Example site

These combination of velocities can be represented by the binary number 10101 which is 21 in decimal. If we apply the FHP-III collision rules to this lattice site we obtain the nontrivial result $21 \rightarrow 42$ (Figure 4).

21 42

Figure 4: Three body, nontrivial collision

Note that the FHP-III rules also state that $42 \rightarrow 21$. All collisions are calculated initially and stored in an array which is used again and again each iteration.

In addition to the one dimensional lattice and collision arrays a six dimensional array which specifies the nearest neighbors of each lattice site in each direction is also necessary. Using such an array makes the implementation of periodic boundaries very easy. A pseudo-code representation of main update function is given in Appendix A.

1.3 Coarse Graining

One disadvantage of using LGCA is that to obtain qualitative results velocities must be averaged over very many sites. This process is known as coarse graining and 16×16 sites and 10 time steps is thought to be the minimum amount of averaging which gives realistic results.

1.4 Macroscopic Equations

The FHP LGCA can be shown to reproduce in the macroscopic limit the Navier-Stokes equation [2, 1]

$$\frac{\partial \mathbf{u}}{\partial t} + (\mathbf{u}\nabla)\mathbf{u} = -\nabla P + \nu\nabla^2\mathbf{u} \tag{1}$$

and the continuity equation

$$\nabla.\mathbf{u} \tag{2}$$

where ν is the (scaled) kinematic shear viscosity. This is related to the microdynamics using the equation

$$\nu = \frac{\nu^{(u)}}{g(\rho_0)} \tag{3}$$

where $\nu^{(u)}$ and $g(\rho_0)$ are the unscaled viscosity and the scaling g-factor respectively.

These quantities depend on the density per cell d and the FHP model being used. Analytical values for FHP-III model are given in Table 5, Appendix B . The speed of sound c_s is also defined for each model. When simulating flow it is important that the flow speed be small compared to the speed of sound so as to obtain subsonic flow. The density per cell d must also be below 0.5 because the scaling factor $g(d)$ vanishes at d=0.5.

1.5 Boundary Conditions

There are several types of boundary conditions used with the FHP LGCA. Figure 5 (a) shows slip boundary conditions where the particles is reflected and Figure 5 (b) shows no slip boundary conditions where the velocity component normal to the

barrier is removed [3]. In addition to slip and no slip periodic boundary conditions may also be used.

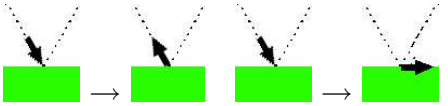

(a) No Slip (b) Slip

Figure 5: Boundary Conditions of the FHP LGCA.

2 Behavior of a Lattice Gas

2.1 Introduction

In this section some of the properties of the lattice gas are investigated. Approach to equilibrium, sound waves, flow through a channel, and flow past a barrier are examined in order to show that lattice gases possess the characteristics of a real fluid.

2.2 Theory

2.2.1 Approach to Equilibrium

A basic property of a gas is that it will fill whatever container into which it is placed. This is in accordance with the Second Law of Thermodynamics; an isolated macroscopic system will evolve to the macrostate of largest entropy and will remain there. Hence if a concentration of lattice gas particles is placed at the centre of an impermeable container and the system allowed to evolve it is expected that these particles would diffuse throughout the container [4].

2.2.2 Sound waves

As was stated previously the FHP model was not the first lattice gas proposed, but was the first lattice gas to possess the correct symmetry to reproduce the Navier-Stokes equation at a macroscopic scale. The FHP lattice gas (unlike the earlier HPP model) is isotropic, a property which will be investigated using sound waves.

2.2.3 Flow Through A Channel

A familiar problem to fluid dynamicists is the laminar flow of fluid through a pipe. Laminar flow in narrow channels is characterized by a streamlined pattern with a parabolic velocity profile. This is called Poiseuille flow after the French scientist who experimented with water flowing through capillary tubes in order to determined how blood flows through the veins of the body [5].

Whether the flow is laminar or turbulent depends upon the Reynolds number which is defined by

$$R_e = \frac{UL}{\nu} \tag{4}$$

where

- U is the characteristic flow speed.
- L is the characteristic spatial scale of the obstacle.
- ν is the kinematic shear viscosity.

Laminar flow occurs at low Reynolds numbers while turbulent flows are associated with high Reynolds numbers. Hence to show the desired effect a slow flow is generated inside a long, narrow channel. It is also essential that the boundary conditions at the top and bottom of the channel are no slip.

2.2.4 Flow Past a Barrier

Another common problem faced in fluid dynamics is the study of flow past a barrier. At small Reynolds numbers the perturbations in the flow are small, at higher values disturbances such as vortices form behind the obstacle, and at higher values still the flow becomes unstable.

When using LGCA to simulate flow past a barrier there is only a limited range of obtainable values for ν and U. The only truly free parameter is L, the size of the obstacle. Hence to perform simulations of flow past a barrier for increasing large Reynolds numbers experiments are performed with increasingly wide barriers.

2.3 Experiment

2.3.1 Approach to Equilibrium

A box containing two compartments (separated by an impermeable wall) was created by placing barrier sites on a lattice. A number of gas particles with zero net momentum were placed at the centre of one of its compartments and the system was allowed to evolved. After the system had reached equilibrium a hole was introduced in the wall separating the two compartments and the system was again allowed to evolve.

2.3.2 Sound wave

A quantity of gas particles were placed on a lattice with periodic boundary conditions and allow to diffuse. Once the system has reached equilibrium a circular overconcentration of particles with zero net momentum was superimposed on the centre of the system. The lattice gas was then allow to evolve.

2.3.3 Flow Through a Channel

A channel was created using a lattice of 1600×160 sites with no slip boundary conditions on the top and bottom edges. Flow was generated by injecting particles at both ends of the channel in such a way that the net flow of particles was from left to right. It was necessary to inject particles in the direction opposite to the net flow so as to reduce the flow velocity as much as possible. With trial and error the following scheme was found to generate the flow velocity $U \approx 0.1$, which was low enough to observe laminar flow.

- Every fourth time step three particles with velocities v_0, v_1 and v_5 were injected at each site on the left-hand side of the lattice.
- Every fourth time step one particle with velocity v_3 was injected at each site on the right-hand side of the lattice.
- Every fifth time step one particle with velocity v_3 was injected at each site on the right-hand side of the lattice.

The simulation was run for 28,500 time steps. Flow velocities were averaged over 16×16 lattice sites and 100 time steps.

2.3.4 Flow Past a Barrier

A lattice was generated with 1920×960 sites with slip boundary conditions on the top and bottom edges. Particles were injected using the following scheme:

- Every fourth time step three particles with velocities v_0, v_1 and v_5 were injected at each site on the left-hand side of the lattice.
- Every fourth time step one particle with velocity v_3 was injected at each site on the right-hand side of the lattice.
- Every ninth time step one particle with velocity v_3 was injected at each site on the right-hand side of the lattice.

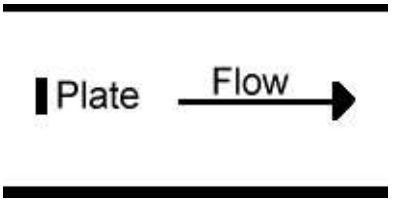

Figure 6: Location of plate in flow.

This generated a flow speed $U \approx 0.15$. Simulations were run with plates of sizes L=20,50 and 80 placed in the flow. The simulations were stopped after 100,000 steps or after the flow had become stable. Flow velocities were averaged over 32×32 lattice sites and 100 time steps.

2.4 Results

2.4.1 Approach to Equilibrium

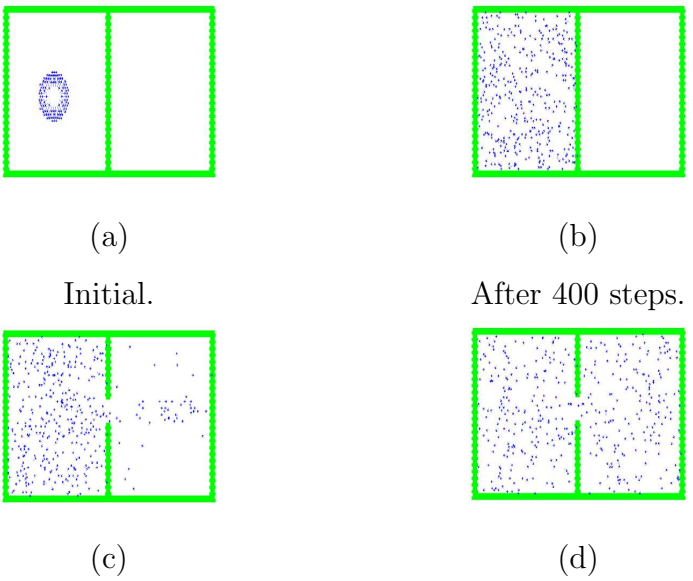

(a) Initial.

(b) After 400 steps.

(c) 100 steps after hole introduced.

(d) 4000 steps after hole introduced.

Figure 7: Diffusion of a lattice gas inside a container. Arrows show the net velocity at each site. Gas particles diffuse inside one compartment and then both compartments. The experiment demonstrates that the lattice gas obeys the Second Law of Thermodynamics, evolving to the macrostate of largest entropy and staying there.

2.4.2 Sound Waves

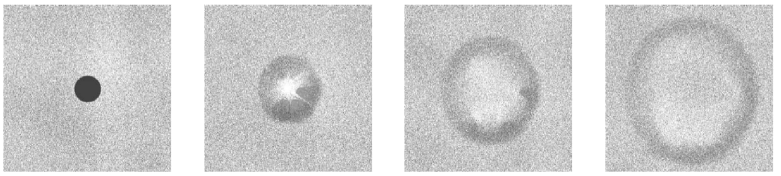

(a) Initial. (b) 70 steps. (c) 140 steps. (d) 210 steps.

Figure 8: Development of a sound wave in an FHP lattice gas due to an overconcentration of particles at the middle of the system. The wave travels isotropically showing no trace of the underlying lattice. The HPP model would fail to do this with the wave traveling faster along the lattice directions.

2.4.3 Flow Through A Channel

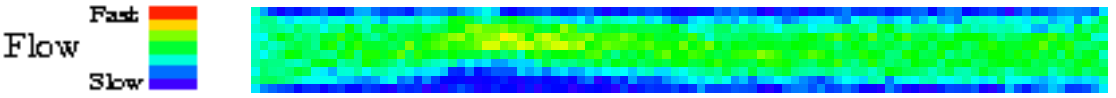

Figure 9: Flow through a channel. Flow speeds generated by coarse-graining over 16×16 sites and 100 time steps are showed using a color gradient. The figure shows the system after 28,500 time steps. Results are noisy but indicate faster flow speeds in the middle of the channel suggesting Poiseuille Flow.

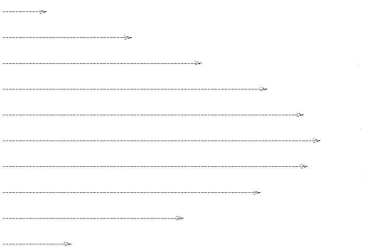

Figure 10: Velocity profile averaged over length of channel. Structure is roughly parabolic consistent with Poiseuille Flow.

2.4.4 Flow Past a Barrier

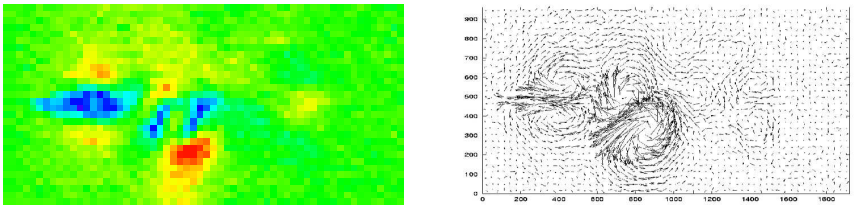

(a) 10,000 steps

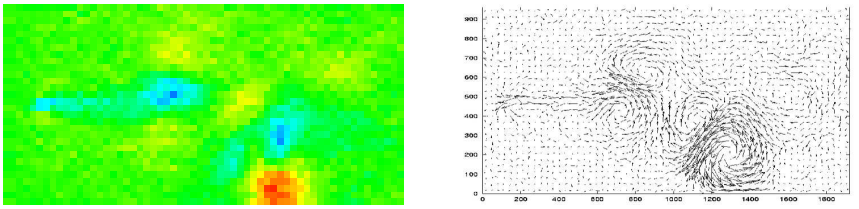

(b) 20,000 steps

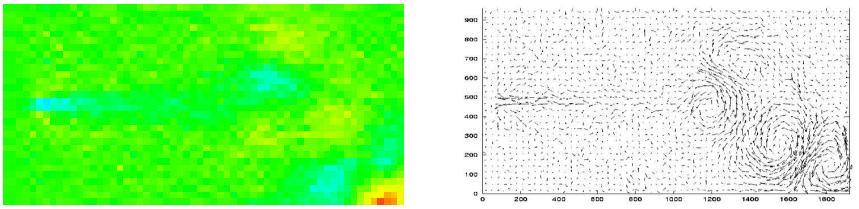

(c) 30,000 steps

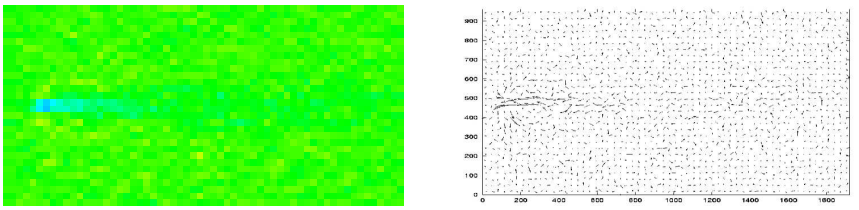

(d) 50,000 steps

Figure 11: Flow past a plate of size L=20. Color gradients indicate flow speeds and vector plots show flow velocities with the mean flow subtracted. Initially the area behind the plate is turbulent, containing vortices and other disturbances. After time these disturbances are carried away and the flow around the plate becomes stable a small wake being the only effect of the barrier.

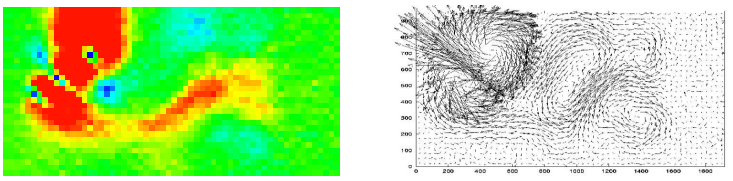

(a) 10,000 steps

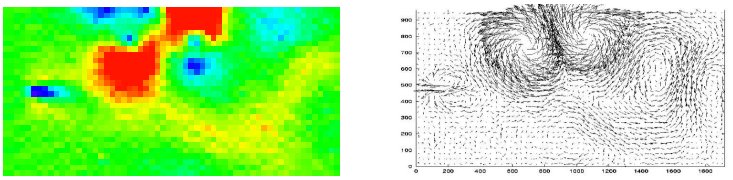

(b) 20,000 steps

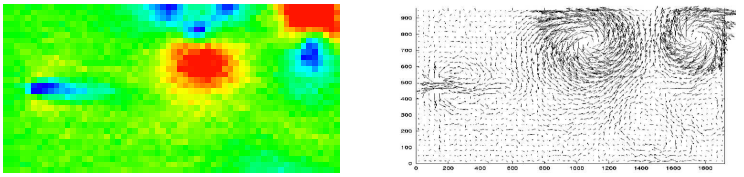

(c) 30,000 steps

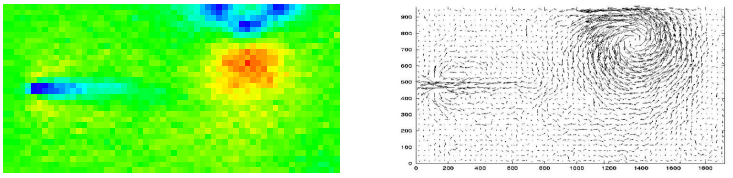

(d) 38,300 steps

Figure 12: Flow past a plate of size L=50. Simulation again suggests initial turbulence and then development of a steady-state. The simulation was cut short and in the final plot a sizable vortex can still be seen. However the area immediately behind the obstacle is stable and shows more significant flow perturbations than the previous simulation with a smaller obstacle. The vector plot suggests that the system is on the verge of forming a stable vortex in the immediate wake of the obstacle.

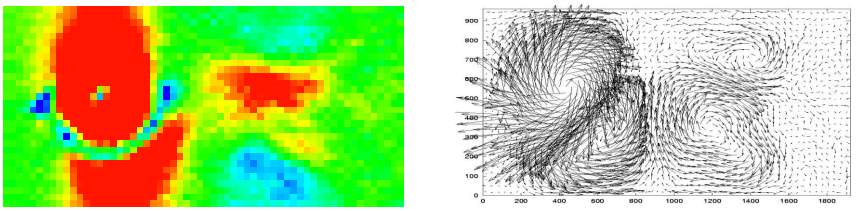

(a) 10,000 steps

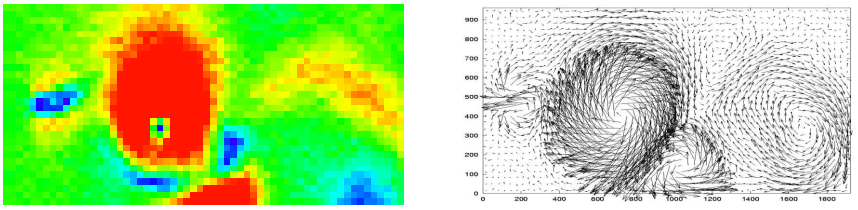

(b) 20,000 steps

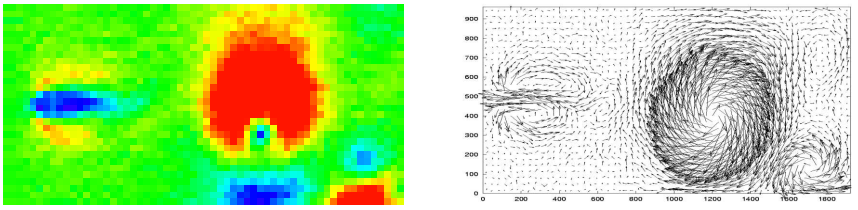

(c) 30,000 steps

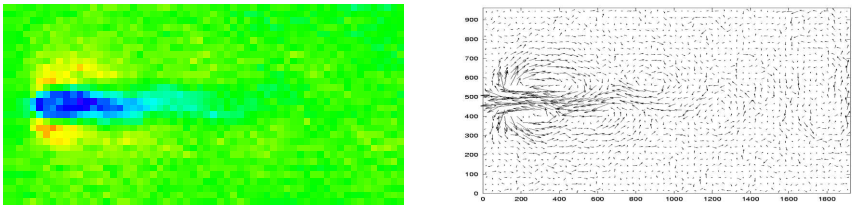

(d) 50,000 steps

Figure 13: Flow past a plate of size L=80. The Reynolds number is increased again and the turbulence increases accordingly. Figure (d) shows that a vortex now exists immediately behind the barrier. The initial turbulence is greater than the previous simulations but disappears as before.

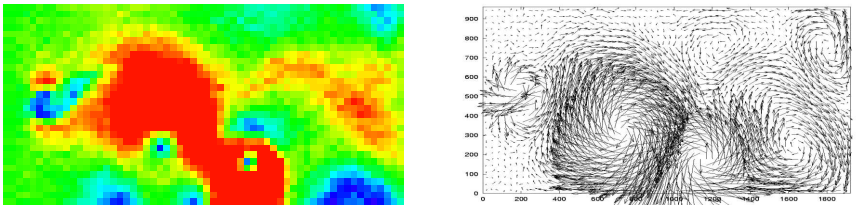

(a) 20,000 steps

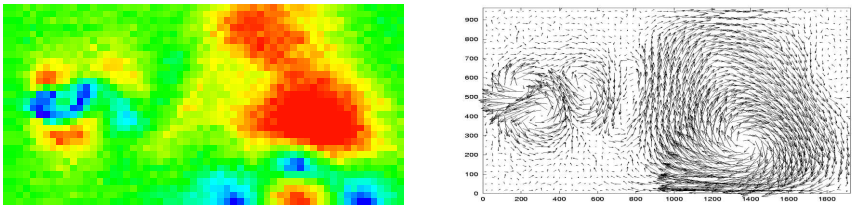

(c) 40,000 steps

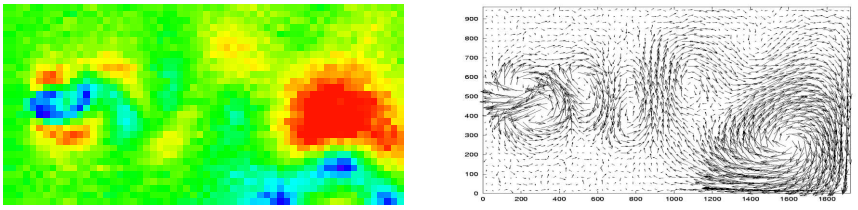

(d) 50,000 steps

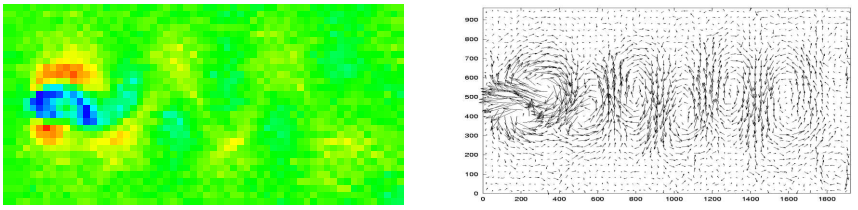

(b) 65,000 steps

Figure 14: Flow past a plate of size L=110. At this even higher Reynolds number the turbulent effects of the barrier after the initial disturbances have passed become very interesting. Figure (d) shows that the barrier is shedding vortices and a so-call von Karman vortex street[3] has built up.

2.5 Discussion

2.5.1 Approach to Equilibrium

Initially the system has all its particles concentrated at the centre of one compartment, Figure 7 (a). This is a very unlikely configuration and the gas evolves to a macrostate of greater multiplicity by diffusing throughout the compartment, Figure 7 (b). By evolving into this state of maximum entropy it is clear that the gas obeys the Second Law of Thermodynamics. A further test is performed by introducing a hole in the wall separating the two compartments. Just after the hole is introduced all the gas particles are located in just one of the compartments. This is a most unlikely state and the gas begins to diffuse from the left hand compartment into the righthand one, Figure 7 (c). There continues to be a net flow of particles into the righthand compartment until the particle densities in both compartments have equilibrated, Figure 7 (d).

2.5.2 Sound waves

Figure 8 (a) shows the initial state of the system, a lattice gas which is diffuse but for an overconcentration at its centre. If the gas is isotopic then its properties should be the same in all directions. By observing the propagation of the sound wave we see that the overconcentration expands out at the same speed in all directions; Figure 8 (b) $\rightarrow$ (d). Hence the speed of sound must be the same in all directions, suggesting that the diffuse gas is indeed isotropic.

2.5.3 Flow Through A Channel

The velocity profile in Figure 10 has parabolic structure reasonably consistent with Poiseuille Flow. It would probably be possible to get closer to the ideal behavior by running the simulation with a longer lattice, minimizing the effects caused by the initial disturbances at both ends of the channel. Figure 9 illustrates one of the big drawbacks of using LGCA, the results are characteristically noisy. Solutions of this problem from other numerical methods would not feature the same amount of noise. It is likely that the clarity of the results in Figure 9 could be improved by averaging over more sites but it very hard to remove the noise altogether.

2.5.4 Flow Past a Barrier

Figures 11 (d) $\rightarrow$ 14 (d) show that in LGCA simulations turbulence increases with the Reynolds number. Figure 11 (d) shows laminar flow, Figures 12 (d) $\rightarrow$ 13 (d) the onset of turbulence, and Figure 14 the shedding of vortices behind the barrier. This qualitative behavior is in good agreement with theory and demonstrates how LGCA simulations of fluid flow can give realistic results.

3 Porous Media

3.1 Introduction

In this section flow through porous media are investigated using the lattice gas. Porous media are generated by randomly placing barrier sites on a lattice through which fluid is passed. Percolation theory is used to investigate how current density depends on porosity. Applications of this method include the flow of oil through a porous rock.

3.2 Theory

3.2.1 Generation of Porous Media

Porous media are created by generating a random number in the interval $0 < r \leq 1$ for every site on a lattice. A site is occupied by a barrier if its random number satisfies the condition $r \leq p$. Clearly the higher the value of p, the smaller the fraction of sites not containing barriers (porosity, ϕ).

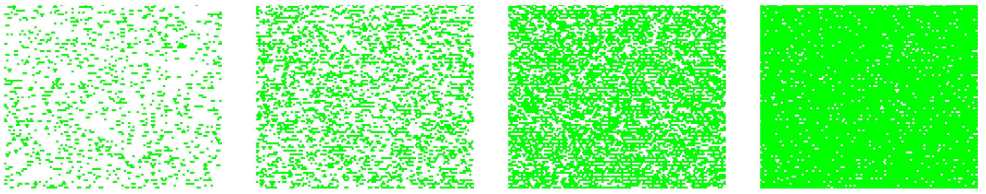

(a)	(b)	(c)	(d)
p=0.1	p=0.25	p=0.5	p=0.9
$\phi = 0.9010$	$\phi = 0.7495$	$\phi = 0.5021$	$\phi = 0.1016$

Figure 15: Porous lattices generated for increasing p, along with their porosity ϕ.

3.2.2 Percolation and Finite Scaling Theory

Consider Figure 15, the higher the value of p used to generate the system the more likely it is that a cluster of barrier sites will form that extends from one edge of the lattice to the other. Such a cluster is called a spanning cluster, the existence of which means that the lattice is impermeable to flow as there is no path from one side of the lattice to the other [1]. Percolation theory states that a well defined critical probability p_c exists such that in the limit of an infinite lattice for $p < p_c$ there will be no spanning clusters and for $p \geq p_c$ there will be one spanning cluster.

The value of p_c depends on the symmetry of the lattice and on its dimension, for a triangular, two-dimensional lattice $p_c = 0.5$. ϕ_c is the porosity of an infinite system generated at p_c and is clearly also equal to 0.5.

The variation of current Σ with porosity ϕ is examined. For a sufficiently large system size this relation is size independent and of the type

$$\Sigma \sim (\phi - \phi_c)^{\mu} \tag{5}$$

Finite scaling theory states that for small lattice sizes or at ϕ_c, we expect size dependent behavior [6]

$$\Sigma \propto L^{-\frac{\mu}{\nu}} \tag{6}$$

where ν is the percolation exponent defined by the critical behavior of the connectedness length $\xi \sim |p - p_c|^{-\nu}$, and here is assumed to be equal to its theoretical value of $\frac{4}{3}$. The current density J is related to current according to

$$J = \Sigma \frac{1}{L} \tag{7}$$

Replacing current with current density in Equation 6 and rearranging gives

$$LJ \propto L^{-\frac{\mu}{\nu}} \tag{8}$$

rearranging gives

$$J = kL^{-\frac{\mu}{\nu}-1} \tag{9}$$

where k is a constant. Taking logs we have

$$\ln J = \ln k + (-\frac{\mu}{\nu} - 1) \ln L \tag{10}$$

Hence to determine μ configurations are generated with $\phi = \phi_c$ for different lattice sizes and the current density is measured for each system.

3.3 Experiments

3.3.1 Diffusion of Particles Through A Porous medium

A porous lattice of size $L = 100$ was generated using the method discussed in Section 3.2.1 with $p = 0.25$. Flow through the porous media created was investigated by injecting particles at the left-hand-side of the lattice and removing them at the righthand-side. The location of the particles after 10, 100, 500 and 1000 time steps was recorded.

3.3.2 Variation of Current Density with Porosity for a Finite System

Lattice configurations of size $L = 100$ we generated for increasing values of p, starting at $p = 0.0$ and moving in steps of 0.001. Particles were injected at the left hand side of each lattice generating flow. The current density (defined as the average of the sum of the horizontal velocity components of the particles that reach the right edge of the lattice) was measured once each system had reached a steady state.

3.3.3 Finite Scaling Determination of Critical Exponent

Porous lattices were generated with $\phi = \phi_c$ for system sizes L=10, 20, 30 ,40, 50, 60 and the steady state currents measured for each. The results were averaged over 100 different lattice configurations for each system size.

3.4 Results

3.4.1 Diffusion of Particles Through A Porous Medium

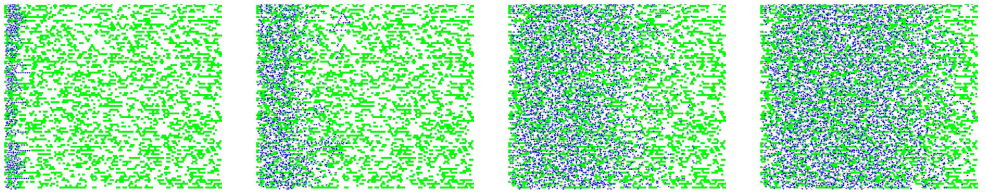

(a) 10 steps (b) 100 steps (c) 500 steps (d) 1000 steps

Figure 16: Diffusion of particles through a porous lattice generated with p=0.25.

3.4.2 Variation of Current Density with Porosity for a Finite System

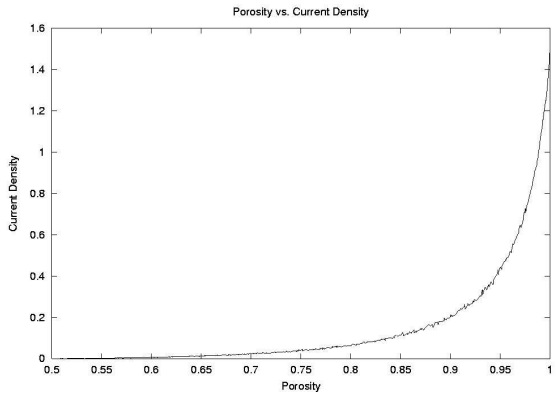

Figure 17: Current density as a function of porosity. Results obtained by generating lattice configurations for increasing values of p, injecting particles v_0, v_1, and v_5 at each site on the left-hand side and measuring steady-state current density on the right-hand side.

3.4.3 Finite Scaling Determination of Critical Exponent

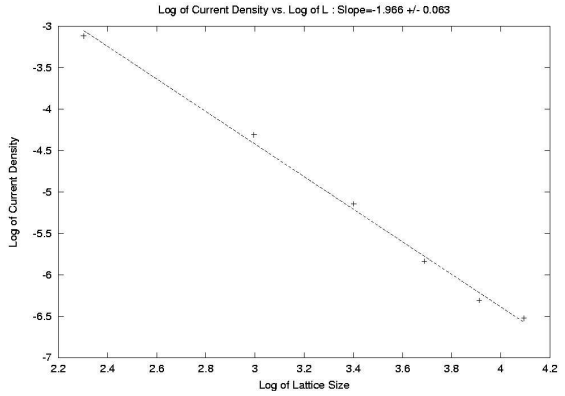

Figure 18: Log-Log plot of current density vs. system size. Lattices are generated with $\phi = \phi_c = 0.5$ for increasing system sizes and the steady-state current density measured for each. Results are averaged over 100 lattice configurations for each system size.

from equation 10 we have for Figure 18

$$slope = -\frac{\mu}{\nu} - 1 \tag{11}$$

using the value obtained for the slope of -1.966 ± 0.063 gives

$$\frac{\mu}{\nu} = 0.966 \pm 0.063 \tag{12}$$

assuming the theoretical value of $\nu = \frac{4}{3}$ yields

$$\mu = 1.288 \pm 0.084 \tag{13}$$

3.5 Discussion

3.5.1 Diffusion of Particles Through A Porous Medium

Figures (a) $\rightarrow$ (d) show the diffusion process of particles across the porous medium. Figure (d) shows the system after 1000 time steps just as the particles have diffused the length of the lattice. If there were no barrier sites present it would take only 100 time steps for particles to reach the far side, which is approximately 10 times quicker than for the medium generated with $p = 0.25$.

3.5.2 Variation of Current Density with Porosity for a Finite System

Figure 17 shows current density as a function of porosity for a system of size $L = 100$. The behavior is not quite of the form of Equation 5 as the system size is finite. However the graph does show current density to be a rapidly increasing function of porosity.

3.5.3 Finite Scaling Determination of Critical Exponent

The critical exponent μ was determined to be equal to 1.288 ± 0.084 which is well within experimental error of the agreed value of 1.3 [6]. The accuracy could perhaps be increased further by averaging over more lattice configurations for each system size.

4 Moving Boundaries, Lattice Gas Bubbles

The flow simulations in section 2.4 are all fixed boundary problems. The size and shape of the obstacle does not change with the flow rate. This section seeks to create boundaries which will change with flow. One such moving boundary problem occurs in foam drainage, where fluid flows predominantly along the plateau borders formed where three films join [7]. These borders are not fixed and can deform due to flow, causing the channels through which the fluid travels to widen [8].

This section will attempt to first construct a single bubble using the lattice gas and moving boundary sites, and then quantitively investigate deformation due to fluid flow.

4.1 Construction of a Lattice Gas Bubble

The central equation governing the shape of soap films is Laplace's Law which in two dimensions is

$$\Delta p = \frac{2\gamma}{r} \tag{14}$$

where ΔP is the pressure difference inside and outside the bubble, r is the radius of curvature and γ is the surface tension. The size of the bubble is determined by two opposing forces; the surface tension which tries to minimize the surface energy and hence the size of the bubble, and the force due to the pressure difference which attempts to push out the bubble boundary.

Although in its derivation Laplace's Law considers a continuous surface, treating a two dimensional bubble as a polygon consisting of a finite number of sides yields the same result.

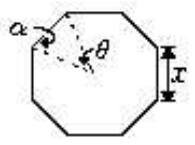

Figure 19: Bubble treated as consisting of a finite number of sides.

The two angles shown on the diagram can be related by

$$\alpha = \frac{\pi - \theta}{2} \tag{15}$$

The angle θ is related to the number of sides N as follows

$$\theta = \frac{2\pi}{N} \tag{16}$$

x the length of any side is given by

$$2r\cos\alpha = x \tag{17}$$

with simple trigonometry it can be shown

$$x = 2r\sin\theta \tag{18}$$

where r (the pseudo radius) is the distance from the centre of the polygon to a point where any two sides meet. Now to derive Laplace's Law all that has to be done is to consider the change $r \to r - \delta r$. The change in the surface energy is

$$\delta U = N(\gamma)2r\sin\theta - N(\gamma)2(r-\delta r)\sin\theta \tag{19}$$

$$\delta U = N(\gamma)2\sin\theta\delta r \tag{20}$$

This must be equal to the work done against the pressure difference given by

$$w = \Delta p N(2r\sin\theta)\delta r \tag{21}$$

Hence the following relationship is obtained

$$\Delta p = \frac{\gamma}{r} \tag{22}$$

As can be seen this relationship differs by a factor of two from Laplace's Law. This is because in a real bubble there are two surfaces separated by a layer of liquid and here only one surface has been considered. Nonetheless it has been shown that a model of a bubble constructed using a finite number of sides can obey Laplace's Law.

In order to recreate the bubble surface within a lattice gas simulation a discrete set of surface points are considered. These points are joined by barrier sites which are tagged with indices registering which side and bubble they belong to. These numbers are stored in the second and third bytes of the lattice integers respectively.

	Bubble Index	Side Index	Lattice Information
Bit	Bits 23→16	Bits 15→8	Bits 7→0

Table 3: Tagging of barrier sites

For example barrier sites connecting point 5 to point 6 in bubble 3 would look as follows

	Bubble Index	Side Index	Lattice Information
Bit	Bits 23→16	Bits 15→8	Bits 7→0
Binary	00000011	00000101	10000000
Decimal	3	5	128

Table 4: Barrier sites belonging to a bubble side

The value stored in the lattice array at these sites is given by the binary number 1100001011000000 or 198,016 in decimal.

By tagging the boundary sites it is possible to register every time a particle strikes off a side (be it from the gas inside or the flow outside). By summing the velocity vectors of the particles which strike each side over time and then averaging the pressure difference at each side P_n is calculated. For the case of a bubble in a vacuum all the pressure is due to the particle inside the bubble and the outward force due to this pressure opposes the pressure due to the surface tension. The point at which sides $n-1$ and n meet is labeled sp_n, the forces at the surface point sp_n can be thought of as follows where

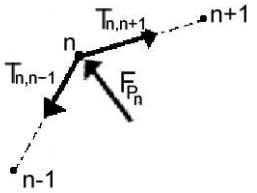

Figure 20: Forces at a surface point n.

- $T_{n,n-1}$: Is a surface tension vector of magnitude γ and in the direction $sp_n\vec{sp}_{n-1}$.
- $T_{n,n+1}$: Is a surface tension vector of magnitude γ and in the direction $sp_n\vec{sp}_{n+1}$.

- F_{p_n} : Is the force due to the pressure, this is taken to be $\frac{1}{2}(P_{n-1}|sp_n sp_{n-1}| + P_n|sp_n sp_{n+1}|)$.

Hence by repeatedly finding the net force on each point and moving them in the direction of this force, a distance proportional to the magnitude, it is possible to obtain equilibrium. Using this model and starting from any arbitrary ring of surface points it should be possible to evolve a two-dimensional bubble.

4.2 Experiment

4.2.1 Surface Energy Minimization

A rectangular arrangement of 32 points was created with an initial separation of 20 lattice units. A surface tension $\gamma = 7$ and an initial concentration of 10647 particles (with zero net momentum) was used. The gas was allow to diffuse inside the bubble for 500 steps and then the surface points were updated every 10 time steps.

4.2.2 Bubbles Attached to a Surface

The model was adapted to simulate a bubble on a solid surface. The simulation was initialized with a rectangular arrangement of points. Three sides of the rectangle (representing the soap film) were given a surface tension, with the remaining side (a barrier to top the perticles escaping) having no tension between the points. The bubble was allowed to evolved over 300 updates of the barrier.

4.2.3 Verification of Laplace's Law

The simulation was run for several values of the surface tension and the steady-state pressure and radius was measured each time. The pressure is taken as the average particle density inside the bubble. The particles were allowed to diffuse inside the bubble for 500 time steps before the surface points were updated every 100 steps and allowed to run for 100,000-200,000 steps (lower surface tension took longer to reach equilibrium). Fewer particles were used in the simulations with lower surface tension so that radius and hence system size would be kept small to allow faster computations. The errors obtained come from the small oscillations in the steady state pressure and radius, these errors become vanishingly small for small surface tensions.

4.3 Results

4.3.1 Surface Energy Minimization

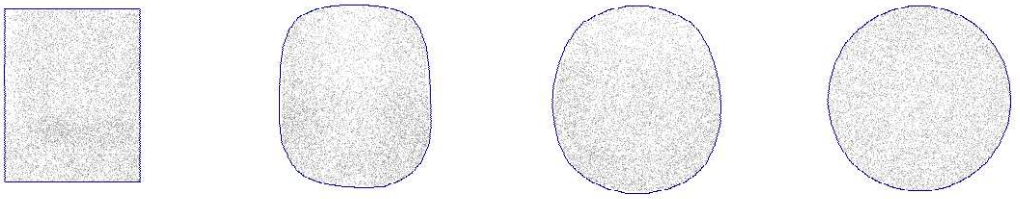

(a) Initial. (b) 5 updates. (c) 10 updates. (d) 50 updates.

Figure 21: Evolution of a 2-D Bubble from Arbitrary Shape. LGCA bubble evolves from the arbitrary rectangular shape to a circle. This is an important agreement with theory, the circle is a surface energy minimum and the tendency of bubbles to minimize their surface energy is one of their most salient characteristics.

4.3.2 Bubbles Attached to a Surface

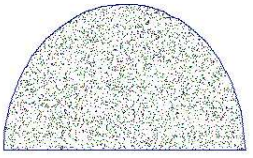

One surface, 300 updates.

Figure 22: Evolution of 2-D Bubble attached to a surface. The curvature of the bubble is circular and the contact angle is ninety degrees.

4.3.3 Verification of Laplace's Law

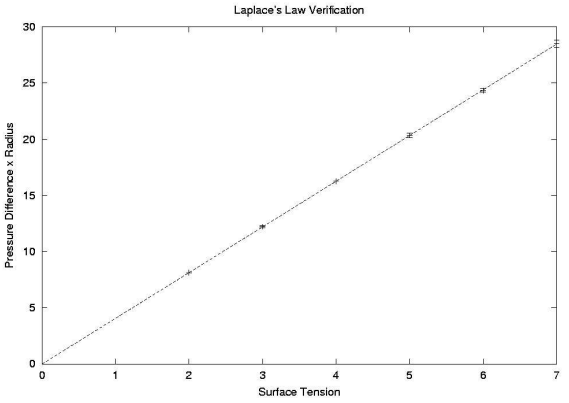

Figure 23: Laplace's Law Verification. Plot of pressure $\times$ radius against surface tension produces a very straight line showing that the LGCA bubble's behavior is consistent with Laplace's Law (14).

4.3.4 Bubble Deformation by Fluid Flow

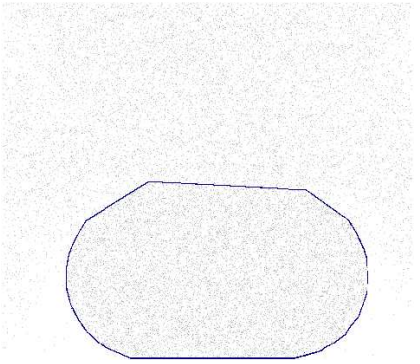

Figure 24: LGCA bubble deformed by fluid flow. Bubble is attached to a solid surface at the bottom of the lattice and allowed to find equilibrium. Flow is then generated by injected particles at the top of the lattice. The resulting bubble shape is not quite symmetric as it is not in the centre of flow. The figure shows one potential problem of the LGCA bubble, when deformed some surface points become very far apart giving parts of the bubble a very flat surface.

4.4 Discussion

4.4.1 Surface Energy Minimization

The bubble transforms in shape from the arbitrary rectangle to a circle (Figure 21). This behavior is important as the bubble has evolved to the surface energy minimum just as a real bubble would. It is interesting that even though only 32 sides were used to construct the bubble the curvature is almost perfectly circular. The imperfections are caused mainly by the bubble existing on a triangular lattice rather than the use of a finite number of sides. If bigger lattices and more sides were used to recreate the bubble these imperfections would be expected to diminish.

4.4.2 Bubbles Attached to a Surface

The simulation was successful in recreating the behavior of a bubble attached to a solid surfaces. Figure 22 shows that is possesses circular curvature and a contact angle of ninety degrees. It was essential to use to the correct boundary conditions for the points where the bubble meets the solid surface and to run the simulation without a film (running along the solid surface) joining these points. Unsuccessful experiments were carried out with the bubble fixed at the points were it meets the surface, this did not produce the correct curvate.

4.4.3 Verification of Laplace's Law

The plot obtained of pressure $\times$ radius against surface tension showed that the LGCA bubble obeyed the linear relationship expressed by Laplace's Law. This result is an important prerequisite to the study of deformation of LGCA bubbles due to flow.

4.4.4 Bubble Deformation by Fluid Flow

Figure 24 suggests that the LGCA could be used to study bubbles deformed by fluid flow, however as can be seen there are problems with the current model. The deformation resulting from the fluid flow has led to some surface points being very far apart making parts of the bubble very flat. A possible solution would be to introduce a new point between two surface points which have become very far apart, hopefully restoring realistic curvature. This method would probably have to be coupled with the removal of surface points which come very close together.

5 Conclusions

It has been shown that lattice gases possess many of the characteristics of a real fluid. Laminar flow through a channel demonstrated Poiseuille flow and the experiments of flow past a barrier showed that the turbulence increased with the Reynolds number. In general the LGCA simulations of fluid flow were found to give realistic if characteristically noisy results.

Flow in porous media and the dependence of current density on porosity was investigated. The critical exponent μ defined by the dependence of the current density J on porosity ϕ was found using finite scaling to be 1.288 ± 0.084 which is in good agreement with the agreed value of 1.3.

An attempt was made to develop a model whereby flow past moving boundaries (specifically the Plateau borders in foams) could be studied. A bubble was constructed using a finite amount of points to recreate the surface tension and a lattice gas the opposing pressure. Experiments showed that such a bubble would minimize its surface energy and obey Laplace's Law. A brief experiment examined how such a bubble could deform due to fluid flow. The results while encouraging showed some limitations of the model, however with further work the author considers it possible for these difficulties to be overcome in which case the model would have some interesting applications. Multiple bubbles could be used to reproduce foam structures and study foam drainage, perhaps demonstrating how the width of channels formed by plateau borders depends on the flow rate.

Overall it has been shown that LGCA are a very useful model the applications of which far exceed traditional fluid flow simulations.

References

[1] Harvey Gould, Jan Tobochnik, *An Introduction to Computer Simulation Methods : Applications to Physical Systems* (1996).

[2] Bastien Chopard and Michel Droz, *Cellular automata modeling of physical systems* (1998).

[3] Dieter A. Wolf-Gladrow, *Lattice-Gas Cellular Automata and Lattice Boltmann Models : An Introduction* (2000).

[4] Ralph Baierlein, *Thermal physics* (1999).

[5] Joseph B. Franzini, E. John Finnemore, *Fluid Mechanics with Engineering Applications* (9th edn, 1997)

[6] Dietrich Stauffer, *Introduction to Percolation Theory* (1985).

[7] Denis Weaire and Stefan Hutzler, *The physics of foams* (1999).

[8] Denis Weaire and Stefan Hutzler, Physica A 257 (1998) 264-274.

A Pseudo-code Representation of Update Function

Main update procedure for FHP LGCA assuming no rest particles and nonslip barrier boundary conditions.

```
Loop over all sites
    Loop over six directions
        if nearest neighbor in the direction -v contains
           a particle with velocity v
            if site does not contain barrier
                translate particle onto lattice site
            else
                reflect particle
            endif
        endif
    Endloop
Endloop

Loop over all sites
    apply collision rules
End Loop
```

B Analytical values for the FHP-III model

	FHP-III
Number of Cells	7
c_s	$\sqrt{\frac{3}{7}}$
$g(d)$	$\frac{7}{12}\frac{1-2d}{1-d}$
$\nu^{(u)}$	$\frac{1}{28}\frac{1}{d(1-d)}\frac{1}{1-8d(1-d)/7)} - \frac{1}{8}$

Table 5: Analytical values for the FHP-III model.